



INTERNATIONAL ATOMIC ENERGY AGENCY  
UNITED NATIONS EDUCATIONAL, SCIENTIFIC AND CULTURAL ORGANIZATION  
**INTERNATIONAL CENTRE FOR THEORETICAL PHYSICS**  
I.C.T.P., P.O. BOX 586, 34100 TRIESTE, ITALY, CABLE: CENTRATOM TRIESTE



SMR.853 - 55

**ANTONIO BORSELLINO COLLEGE ON NEUROPHYSICS**

**(15 May - 9 June 1995)**

---

**"Sensorimotor Encoding by Synchronous Neural Ensemble  
Activity at Multiple Levels of the Somatosensory System"**

**Miguel A.L. Nicolelis**  
**Department of Neurobiology**  
**Duke University Medical Center**  
**Durham, NC 27710**  
**U.S.A**

---

**These are preliminary lecture notes, intended only for distribution to  
participants.**

# Sensorimotor Encoding by Synchronous Neural Ensemble Activity at Multiple Levels of the Somatosensory System

Miguel A. L. Nicolelis,\*† Luiz A. Baccala, Rick C. S. Lin, John K. Chapin

Neural ensemble processing of sensorimotor information during behavior was investigated by simultaneously recording up to 48 single neurons at multiple relays of the rat trigeminal somatosensory system. Cortical, thalamic, and brainstem neurons exhibited widespread 7- to 12-hertz synchronous oscillations, which began during attentive immobility and reliably predicted the imminent onset of rhythmic whisker twitching. Each oscillatory cycle began as a traveling wave of neural activity in the cortex that then spread to the thalamus. Just before the onset of rhythmic whisker twitching, the oscillations spread to the spinal trigeminal brainstem complex. Thereafter, the oscillations at all levels were synchronous with whisker protraction. Neural structures manifesting these rhythms also exhibited distributed spatiotemporal patterns of neuronal ensemble activity in response to tactile stimulation. Thus, multilevel synchronous activity in this system may encode not only sensory information but also the onset and temporal domain of tactile exploratory movements.

The processing of somatosensory information in the mammalian brain involves the transmission of neural activity from the skin to the neocortex by way of parallel pathways that ascend through a hierarchical sequence of neural structures (1). Like those in other sensory systems, these ascending pathways are far outnumbered by corticofugal descending projections (2), which can act at multiple subcortical levels to modify the processing of sensory information (3). These connections define a recurrent network that is theoretically capable of generating complex emergent dynamic patterns of neural activity, manifested by synchronous oscillations or even chaotic behavior (4), that could be computationally useful (5). The existence of this network raises the question of whether large-scale coordinated activity of neural ensembles involving multiple levels of a sensory system (that is, brainstem, thalamus, and cortex) can play a fundamental role in the coding of sensory information. To address this issue, we simultaneously recorded up to 48 single neurons, distributed across up to five distinct processing relays of the trigeminal somatosensory system, in freely behaving rats (6). The rat trigeminal system is a multilevel, recurrently interconnected neuronal net-

work, specialized for processing complex patterns of tactile stimuli generated by the repetitive contacts of facial whiskers with surrounding objects. Rats rely on rhythmic movements of their facial whiskers, much as humans rely on coordinated movements of their fingertips, to discriminate object shape and texture (7). Although the properties of single neurons belonging to this sensory system have been well studied under anesthetized conditions (8), little is known about information processing at the neural ensemble level during exploratory tactile behaviors.

The results described here are based on the long-term behavior of 424 single neurons chronically recorded in 11 animals. Sampled structures included the trigeminal ganglion (Vg, 17 cells), the principal (PrV, 52 cells) and spinal (SpV, 39 cells) trigeminal brainstem nuclei, the ventral posterior medial (VPM, 186 cells) and posterior medial (POm, 19 cells) nuclei of the thalamus, the primary somatosensory (SI, 95 cells) cortex, and the primary motor (M1, 32 cells) cortex. Pairwise cross-correlation analysis was initially used to characterize the coordinated activity of simultaneously recorded neurons across the trigeminal system. Cross-correlograms averaged around the spiking of a single representative VPM neuron (Fig. 1A) in each animal demonstrated the existence of synchronous oscillatory discharge (7 to 12 Hz) in 98% of the ipsilateral VPM neurons, 92% of the ipsilateral SI cortical neurons, and 49% of the contralateral SpV neurons recorded in this study. During episodes of synchronous firing, thalamic neurons tended to phase-lag (follow) cortical neurons (Fig. 1A) by time periods ranging from 0 to 20 ms (mean  $\pm$

SD,  $9.19 \pm 4.67$  ms;  $n = 84$  SI-VPM pairs in six animals). The regular progression of these lags across evenly spaced electrode arrays implanted in the SI cortex (for an example see the bottom third of Fig. 1A) was compatible with a traveling wave of neuronal activity crossing this cortical region. Similar synchronous oscillations were also observed among neurons in the whisker representation of the rat M1 cortex, and, like the SI cortical neurons, these neurons phase-led neurons in the VPM thalamus. The simultaneously recorded neurons in the brainstem SpV nucleus were also synchronized with this oscillation, and these neurons phase-led neurons in the VPM thalamus by as much as 40 ms (Fig. 1A). By contrast, neurons within the VPM and POm thalamus exhibited remarkably synchronous firing with minimal phase lags ( $<3$  ms). This high degree of synchrony was observed bilaterally in the thalamus, implying that all of these thalamic structures were simultaneously entrained into the oscillations.

The possibility that these oscillations were caused by rhythmic sensory feedback resulting from active whisker movements (WMs) was ruled out by three observations. First, as detailed below, they began well before the onset of WMs. Second, the same pattern of oscillations was clearly present in adult animals subjected to complete unilateral whisker removal or facial nerve section in early development (9). Third, the oscillations were not observed in either the first-order (Vg) or the primary second-order (PrV) sensory relays in this pathway.

To further examine the neurophysiological properties of the simultaneously recorded multilevel neural ensembles, we developed analytical techniques for representation of neuronal population functions. We used principal component analysis (PCA) to construct continuous representations of the activity of neuronal populations by weighted summation of the time-integrated activity of all neurons (10). We observed that reconstructions of the first principal component (PC1), derived from combined cortical, thalamic, and brainstem neural ensemble activity, more reliably identified the existence and time course of oscillatory episodes than did the raster displays of single neuronal spiking (Fig. 1B). This difference was due to the marked variability in spiking patterns (timing and number of spikes) of single neurons over different oscillatory cycles. Indeed, only a fraction of the population fired during a particular cycle. Thus, oscillations revealed in PC1 were not completely defined by any one neuron but instead drew small amounts of variance from each of a large population of neurons. Because PC1 normally explains the most global sources of covariance between variables, it is significant that it tended to be domi-

M. A. L. Nicolelis, R. C. S. Lin, J. K. Chapin, Department of Anatomy and Neurobiology, Medical College of Pennsylvania and Hahnemann University, Philadelphia, PA 19102, USA.

L. A. Baccala, Department of Electrical Engineering, University of Pennsylvania, Philadelphia, PA 19104, USA, and Department of Electronic Engineering, University of São Paulo, São Paulo, SP, Brazil.

\*Present address: Department of Neurobiology, Box 3209, Duke University Medical Center, Durham, NC 27710, USA.

†To whom correspondence should be addressed.

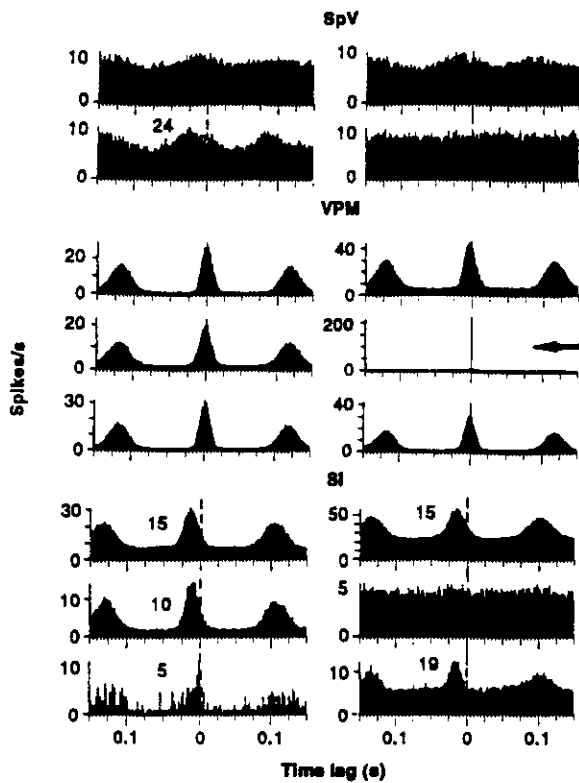
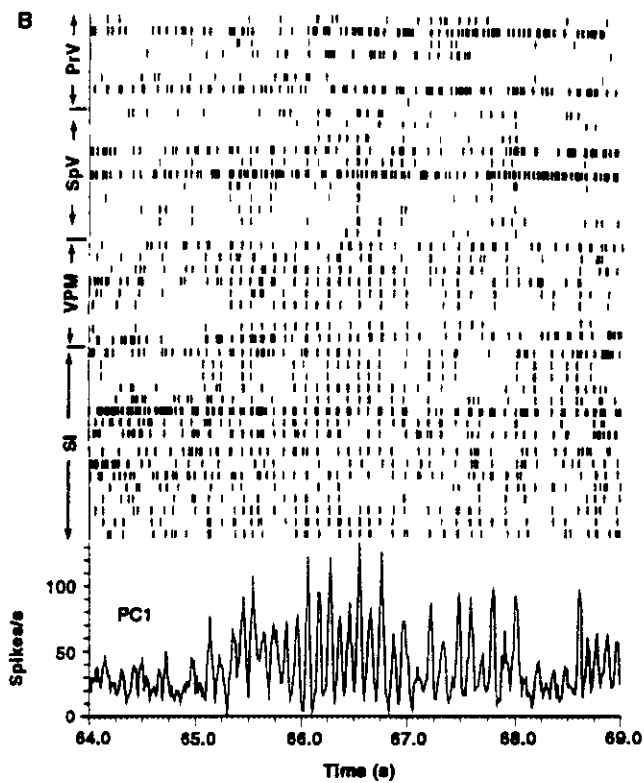


**Fig. 1.** Spontaneous 7- to 12-Hz oscillations at multiple relays of the trigeminal somatosensory system. (A) Cross-correlograms (CCs), calculated for 16 out of a total 48 simultaneously recorded neurons, reveal synchronous 7- to 12-Hz oscillations at three levels of the trigeminal pathway (SpV, 4 neurons; VPM, 6 neurons; and SI, 6 neurons). All CCs centered around the spiking of one reference VPM neuron (autocorrelation shown at arrow). Numbers on top of CCs indicate the time interval (in milliseconds) by which each SpV or SI neuron phase-leads the reference VPM neuron. All horizontal axes indicate



pre- and post-VPM spike times (in seconds), VPM spiking occurred at 0.0 s, as indicated by the vertical dashed lines. Vertical axes of CCs indicate equivalent firing rates per bin (bins: 1-ms duration). (B) Continuous strip chart showing 43 single-unit rasters and reconstructed PC1 (bottom) over the same 5.0-s time period in an awake rat. The rasters show spiking activity of simultaneously recorded neurons in four system relays; PV, SpV, VPM, and SI. Not shown are the five neurons recorded in Vg, which were inactive over this period. The vertical axis depicts the weighted neuronal population firing rate.

nated by these widespread synchronous oscillations (11).

Spectrum analysis of the time series representing PC1 for the multilevel data demonstrated that the most important power contribution of the oscillations was in the frequency band from 7 to 12 Hz, with a secondary peak at 19 to 21 Hz. The oscillations appeared in episodes ranging from 0.8 to 38.2 s (mean  $\pm$  SE,  $3.96 \pm 0.3$  s;  $n = 196$  episodes) and were closely associated with preparation for <sup>WT</sup> movements (Fig. 2). Although they always began during complete immobility (Fig. 2A), in 79.1% (155 of 196, from five animals) of the recorded episodes, these oscillations predicted with a high degree of statistical confidence ( $P < 10^{-6}$ ) the imminent onset of low-amplitude whisker-twitching (WT) movements (12). Even though WT began on average  $581 \pm 45.2$  ms after the oscillation onset, the distribution of these latencies was markedly skewed, such that 62.5% of all WT episodes began during the first 500 ms. The frequency range of WT (7) closely matched the frequency of neural oscillations in the trigeminal system (7 to 12 Hz). In fact, after

the onset of WT, these oscillations assumed a phase-locked relation with <sup>WT</sup> movements: Oscillatory peaks in the SpV neurons were synchronous with the early phase of whisker protraction, whereas peaks in the SI and VPM neurons were synchronous with the middle and late phases of whisker protraction, respectively (Fig. 2B). Subsequent onset of high-amplitude rhythmic exploratory WMs, which were often combined with head movements or locomotion, always induced a cessation of these oscillations. In the absence of WT, head movements (HMs) alone were never preceded by oscillations (see HMs starting at 13.7 s in Fig. 2A). Independent reconstruction of principal components (PCs) at different levels of the trigeminal pathway revealed that in 79.8% (138 of 173,  $n =$  five animals) of the oscillatory sequences, rhythmic activity clearly began in the SI cortex (Fig. 3A, point a) and progressed to the VPM thalamus (Fig. 3A, point b). Neurons in the SpV tended to be recruited last, exhibiting clear rhythmic activity  $1.53 \pm 0.07$  oscillatory cycles ( $\sim 100$  ms per cycle) before the onset of WT (as indicated by the dashed line), as

averaged across 114 episodes in which SpV neurons were recorded (Fig. 3A, point c). Although the SpV neurons were the last to be recruited into rhythmic activity, after the onset of WT they phase-led both the SI and VPM neurons (Figs. 2B and 3B). This observation argues against a simple pacemaker mechanism for these oscillations.

The classification of this oscillatory phenomenon remains elusive (13). Its association with attentive behaviors resembles that of "mu" rhythms recorded in humans (14) and the "sensorimotor" rhythms described in cats and primates (15). Our data suggest that similar oscillatory activity is present at multiple processing levels of the rat somatosensory system and that it can be definitively related to a specific type of rhythmic movement (WT). Differences in the frequency of this rhythm across species might therefore be related to different time domains of movements for which it is preparatory. Our hypothesis is that the 7- to 12-Hz frequency component of the oscillations defines an "internally generated representation" of the sensorimotor temporal domain of exploratory <sup>WT</sup> movements, especially

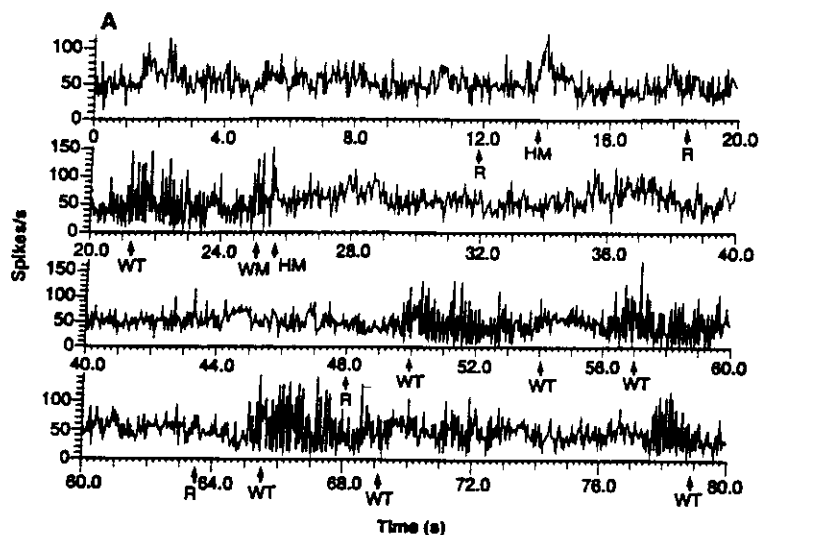


**Fig. 2.** Association between oscillations and WT behavior. (A) Four strip charts depicting 80.0 s of continuous activity of PC1, reconstructed from the activity of 48 neurons recorded at five levels of the trigeminal pathway. This PC1 shows several episodes of synchronous 7- to 12-Hz oscillations. Frame-by-frame analysis of video tape synchronized to this experiment showed that these oscillations were associated with a distinctive succession of behaviors, beginning with rest (R), followed by low-amplitude WT, and ending with high-amplitude exploratory WMs, which were often associated with HMs. For example, after a period of intermittent movement, the animal assumed an immobile attentive posture (R) at 18.5 s, which continued until the onset of oscillations (7 to 12 Hz) at 20.5 s. About 500 ms later, a sequence of low-amplitude WT (21.2 to 25.1 s) began. This WT was then followed by WM and HM, which terminated the oscillations. Vertical arrows mark the onset of various behaviors. (B) Phase synchronization between whisker protraction and 7- to 12-Hz oscillations at multiple levels of the trigeminal system. A raster plot (top) and PC1s (for different levels) are shown centered around the onsets of 64 episodes of whisker protraction during WT. Each black horizontal line in the raster defines the time period between protraction onset (vertical dotted line at 0.0 s) and subsequent retraction onset. The horizontal dotted line depicts the average duration (49 ms) of whisker protraction during continuous WT. The PC1s calculated for all levels together (topmost PC1 plot) or for each individual level (SpV, VPM, and SI) are averaged around the onset of whisker protraction. All PC1s are tightly phase-locked to whisker protraction, and the SpV, SI, and VPM activity peaks occur during the early, middle, and late phases of protraction, respectively. The vertical axis depicts the weighted neuronal population activity.

quences during spindling occurred in much shorter (0.4 to 1.2 s) and stereotyped episodes than did the sensorimotor rhythm described during awake immobility. Third, unlike the relatively constant amplitude of the sensorimotor oscillations, the spindle exhibited very characteristic waxing and waning wave patterns. Finally, spindle episodes recurred every 5 to 10 s, whereas the occurrence of sensorimotor rhythms was linked to behavior changes and was therefore more random. Thus, although spindle involved similar frequencies (7 to 14 Hz) and were observed in the same thalamocortical circuits, they clearly subserve a very different functional role from the sensorimotor rhythms described here.

To further define the dynamic nature of sensory processing among the multiple processing levels of the rat trigeminal system during awake immobility, we carried out repetitive stimulation of single whiskers in the same animals. Population poststimulus time histograms (PPSTHs) were used to represent the simultaneously recorded sensory responses of the same ensemble of neurons to repeated stimulation of a given whisker (Fig. 4). This analysis revealed that Vg and PrV neurons (1 to 13 in the vertical scale of Fig. 4) responded well to the stimulation of whisker B4 (Fig. 4B) but exhibited little or no response to stimulation of other sites, such as whisker B2 (Fig. 4A) and fur rostral to B4 (Fig. 4C). In contrast, most of the SpV (14 to 22), VPM (23 to 31), and SI (32 to 47) neurons displayed statistically significant ( $P < 0.01$ ) responses to all three stimulation sites. In the ascending progression from Vg to SI, the latencies to the initial response increased from 2 to 8 ms. In addition, secondary long-latency responses were evident through much of this system, appearing first in a few PrV neurons and becoming more prominent and longer in latency at higher levels. For instance, thalamic cells exhibited secondary long-latency responses up to 35 ms, and, in the SI cortex, secondary long-latency responses ranged from 20 to 70 ms after the stimulus. As previously demonstrated for the VPM neurons (17), these results showed that sensory maps at most levels of the trigeminal system (SpV, VPM, POm, and SI) were defined by complex spatiotemporal patterns of neural ensemble responses. Therefore, although the Vg and PrV structures contained relatively simple topographic sensory representations and did not exhibit pre-movement oscillations, structures that manifested synchronous oscillations (SpV, VPM, POm, and SI) exhibited distributed (18) and dynamic somatosensory maps.

The complex spatiotemporal structure of these maps may result from asynchronous interactions between feedforward and feedback projections at each level of this sys-

WT, which is disseminated across much of the somatosensory pathway before the onset of ~~WT~~ <sup>the movement</sup>. We propose that this ~~behavior~~ <sup>facilitation function</sup> provides a phasic sensory facilitation function timed to coincide with the ~~protraction phase~~ <sup>whisker</sup> of WMs, which is known to be the period in which active sampling of tactile information occurs in rats (7). In this model, the observed 19- to 21-Hz frequency component might constitute a representation of the timing of alternating subphases of WM—for example, protraction and retraction (Fig. 2B). Further support for this model is provided by our observation that, depending on the oscillatory phase at which

the incoming sensory volley arrives, these rhythms can exhibit several patterns (Fig. 3C).

The strong correlation of these sensorimotor rhythms with immobile attention leading to ~~WT~~ <sup>clearly distinguishes</sup> these rhythms from other brain rhythms such as spindling (16). To further clarify this distinction, we compared the sensorimotor rhythms with spindling activity in the same animals and found that there were several ~~distinctions~~ <sup>distinctions</sup> between these two rhythms. First, spindles occurred during drowsiness (as opposed to attentive resting) and during the initial stages of sleep, in the complete absence of WMs. Second, oscillatory se-

DIFFERENCES

3.

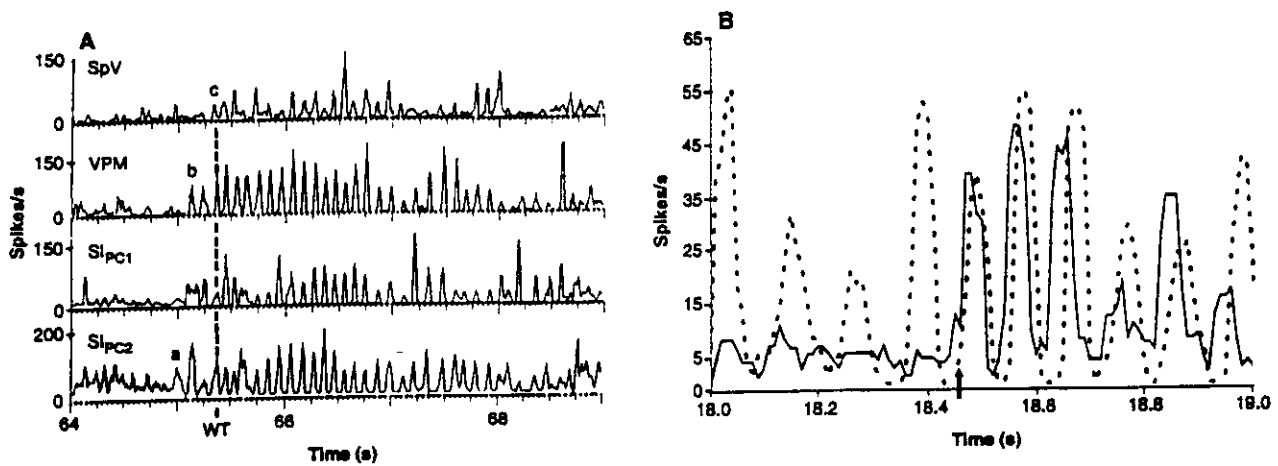


**Fig. 3.** (A) Oscillations appear first in the SI cortex. Four strip charts show four PCs derived independently from simultaneously recorded neurons in specific nuclei: SpV (11 neurons), VPM (8 neurons), and SI (16 neurons). For SI, both PC1 and PC2 are shown. Oscillatory peaks begin in the SI neurons (a), spread to the VPM neurons (b) after one to two cycles, and finally reach the SpV neurons (c) after five to six cycles. (B) Strip charts depicting the PCs for the SpV neurons (dark line) and the VPM neurons (dotted line) show that in the VPM neurons, oscillations are continuous for more than four cycles before recruitment of the SpV neurons into the oscillations. Nevertheless, the SpV neurons clearly phase-lead the VPM neurons thereafter. The recruitment of the SpV neurons coincides with the onset of WT movements (vertical arrow). (C) Nonlinear interactions between 7- to 12-Hz oscillations and single-whisker stimulations are represented by a series of four strip charts, each depicting 2.5-s sequences of PC1 derived from 23 VPM neurons. Single-whisker stimulation trials (vertical bars, circled numbers) superimposed on the PC1 record show that sensory stimulation can terminate ongoing oscillations (1), modify the phase of the oscillations (2, 5, and 6), produce an isolated sensory response (3), initiate oscillations (4 and 8), have no effect (7 and 10), and augment the oscillation peak (9). The vertical axis depicts the weighted neuronal population firing rate.

tem. As a consequence, the coding of sensory information in most cortical and sub-cortical relays of the trigeminal pathways occurs at the ensemble rather than at the single-unit level and involves both spatial and temporal domains. According to this scenario, topographic maps defined in anesthetized animals represent only a first approximation of the system's functional organization. In the awake condition, however, spatiotemporal complexity substitutes for topography as the main strategy for the coding of sensory information.

These results indicate that the functional organization of the rat somatosensory system is fundamentally linked to the coordinated activity of large ensembles of neurons, distributed through multiple levels of the brain. Dynamic patterns of neural ensemble activity in this sensory system were found not only to code tactile stimulus attributes but also to anticipate the occurrence of stereotyped WT behaviors associated with active tactile exploration of the surrounding environment. Because these oscillations appear to mimic a motor output function, they are consistent with earlier demonstrations in rats, cats,

and monkeys that the transmission of sensory information through different levels of the somatosensory system is strongly modulated as a function of the phase of active movement (19).

#### REFERENCES AND NOTES

1. J. H. Kaas, in *The Human Nervous System*, G. Paxinos, Ed. (Academic Press, San Diego, CA, 1990), pp. 813-844.
2. S. M. Sherman and C. Koch, in *The Synaptic Organization of the Brain*, G. M. Shepherd, Ed. (Oxford Univ. Press, New York, 1990), pp. 246-278; I. T. Diamond and W. C. Hall, *Science* **164**, 251 (1969); J. Cmielowska, G. E. Carvell, D. J. Simons, *J. Comp. Neurol.* **285**, 325 (1989).
3. H. -C. Shin and J. K. Chapin, *Brain Res. Bull.* **22**, 245 (1989); *ibid.* **24**, 257 (1990); *Neurosci. Lett.* **108**, 116 (1990).
4. W. J. Freeman, *Mass Action in the Nervous System* (Academic Press, New York, 1975); \_\_\_\_\_ and B. Baird, *Behav. Neurosci.* **101**, 393 (1987); G. Laurant and H. Davidowitz, *Science* **265**, 1872 (1994).
5. H. Sompolinsky, D. Golomb, and D. Kleinfeld [*Phys. Rev. A* **43**, 6990 (1991)] have suggested that computations might be carried out by systems of coupled oscillators in which information is carried in changing patterns of synchronous coupling between these oscillators. Computation in Hopfield nets [J. Hopfield, *Proc. Natl. Acad. Sci. U.S.A.* **79**, 2554 (1982); \_\_\_\_\_ and D. W. Tank, *Science* **233**, 625 (1986)], which are recurrently connected artificial neural networks, involves a dynamic evolution

of the system toward a steady state.

6. Eleven adult Long-Evans (hooded) rats (250 to 300 g) were used in this study. Surgical and recording procedures complied with NIH-ALAC recommended procedures for animal use and care. These procedures and methods for single-whisker stimulation and data analysis are fully described elsewhere [M. A. L. Nicolais and J. K. Chapin, *J. Neurosci.* **14**, 3511 (1994)]. Briefly, bundles and arrays of 50- $\mu$ m microwires (NBLABS, Dennison, TX) were implanted under pentobarbital anesthesia (50 mg per kilogram of body weight, intraperitoneal). Sets of 8 to 16 microwires were stereotaxically placed in up to five neuronal structures per animal. Teflon-coated stainless steel wires (0.007 inch) were also implanted in multiple facial muscles to obtain EMG signals. Concomitant videotaping of the animal's activity was also used to define the timing of different behaviors and to correlate these events with patterns of ensemble activity. Recordings were obtained during awake immobility, active whisker exploration of the environment, locomotion, and sleep. We obtained synchronous recordings of neuronal, EMG, and video signals with the use of a multichannel neuronal processor (MNAP; Spectrum Scientific, Dallas, TX). A single computer clock (accuracy, 0.2 ms) was used to synchronize the acquisition of neuronal and video data. Each video field was stamped with the elapsed time in hundredths of a second. A Lafayette (Lafayette, IN) Super VHS video analysis system was used for post hoc field-by-field analysis of video recordings. The 60 field per second video sampling rate provides a 16.7-ms temporal resolution, and the synchronization with experimental data capture has a 10-ms resolution. In the ensemble data analysis we used the following computer programs: Analyze (J. K. Chapin); Strang-

ELECTROMYOGRAMS (EMGs)

4colorfig004

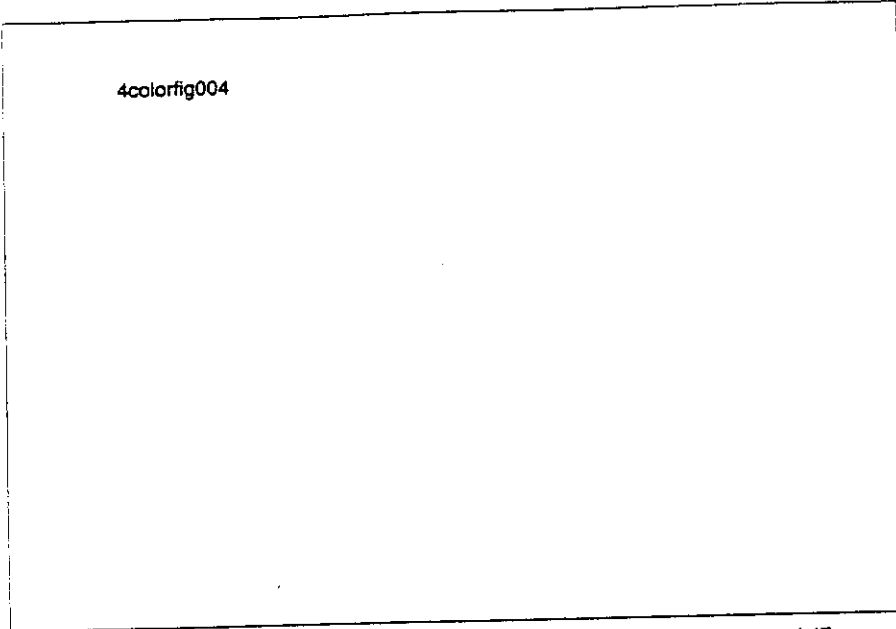


**Fig. 4.** Color-coded PPSTHs depicting the spatiotemporal sensory response patterns of 47 neurons simultaneously recorded across five levels of the trigeminal system in an awake rat. The absolute neuronal firing intensities are displayed through a seven-color contour plot [dark red, highest firing rate (up to 120 Hz); dark blue, lowest firing rate (as low as 0 Hz)]. Neurons that are included in this multilevel ensemble are organized in the vertical axis (Vg, 1 to 4; PrV, 5 to 13; SpV, 14 to 22; VPM, 23 to 31; and Sl, 32 to 47). Poststimulus time is represented in 5-ms time bins numbered from 1 to 10 (0 to 50 ms). The graphs were produced by calculating the intensities of spike discharge of each neuron within the simultaneously recorded ensemble, rank-ordering the neurons into rows according to receptive field location, and then plotting the data into a color-coded contour plot image. Each PPSTH depicts the spatial extent and timing of the spread of sensory responses through the nuclei in which neuronal ensembles were simultaneously recorded. Sensory responses obtained for whisker B2 (A), whisker B4 (B), and fur rostral to B4 (C) are illustrated. All PPSTHs were based on 360 single-whisker stimulation trials. Each trial consisted of a 100-ms step pulse that produced a 3° whisker deflection (upward first). Raw data were smoothed with a spline algorithm (Matlab); the statistical significance of sensory responses was computed by means of a one-way Kolmogorov-Smirnov test.

er (Biographics, Winston-Salem, NC); CSS:Statistica (Statsoft, Tulsa, OK); and Matlab (Mathworks, Natick, MA).

7. G. E. Carvell and D. J. Simons, *J. Neurosci.* 10, 2638 (1990).  
 8. J. K. Chapin and R. C. S. Lin, *J. Comp. Neurol.* 229, 199 (1984); J. K. Chapin, *Exp. Neurol.* 82, 549 (1986); M. Armstrong-James and C. A. Callaghan, *J. Comp. Neurol.* 303, 211 (1991).  
 9. R. C. S. Lin, M. A. L. Nicolelis, M. E. Diamond, J. K. Chapin, *Soc. Neurosci. Abstr.* 19, 106 (1993); M. A. L. Nicolelis, R. C. S. Lin, J. K. Chapin, *ibid.* 20, 125 (1994).  
 10. PCA simplifies the analysis of the activity of large numbers of neurons by linearly combining their co-

variant activity over a large number of experimental time bins into a much smaller number of PCs that are responsible for most of the covariance. The matrix of coefficients for axis rotation that defines each PC is then used to weight-sum the simultaneous time-integrated activities of all neurons into a single continuous "population function," which provides optimal identification of moment-to-moment changes in the activity of the underlying "factor" defined by the PC. For example, we constructed the record in Fig. 1B by (i) dividing the 1813-s experiment into 181,300 10-ms time samples; (ii) measuring the spiking of each of the 48 simultaneously recorded neurons within each time sample; (iii) standardizing each data sample by subtracting the mean and dividing by the standard

deviation; (iv) using these samples to construct a 48-by-48 covariance matrix; (v) performing PCA on this matrix; and (vi) using the PC1 eigenvector to weight-sum all the standardized data samples into a continuous population function, consisting of a time series containing a single data point for each 10-ms time bin in the experiment.

11. In contrast to the information derived from PC1 higher-order components (with successively lower eigenvalues) identified local sources of covariance including phase differences between oscillations at different levels of the pathway and specific sensor information.  
 12. Chi-square analysis rejected the null hypothesis (there is no temporal relation between WT and th oscillations. This analysis involved comparing the experimentally derived distribution of WT onset time (quantized in 100-ms bins after the onset of oscillation) with the theoretical distribution of onset time that would be predicted by the null hypothesis (that is, a homogeneous distribution whose sum of counts equals the experimental sum). Because the experimental distribution was markedly skewed toward very short time delays after the onset of oscillation, very high  $\chi^2$  was obtained (658; df = 32 bins), allowing rejection of the null hypothesis ( $P < 10^{-9}$ ).  
 13. K. Semba, H. Szechtman, B. R. Komisaruk, *Brain Res.* 195, 281 (1980); K. Semba and B. R. Komisaruk, *Neuroscience* 12, 761 (1984); G. Buzsaki, *ibid.* 41, 351 (1991).  
 14. H. Gastaut, *Rev. Neurol. (Paris)* 87, 176 (1952); Kristeva-Feige et al., *Neuroreport* 4, 1291 (1993); Salmelin and R. Hari, *Neuroscience* 60, 537 (1999).  
 15. A. Rougeul, J. J. Bouyer, L. Dedet, O. Debray, *Epileptologia*, *Clin. Neurophysiol.* 48, 310 (1997); A. Rougeul, J. J. Bouyer, M. F. Montaron, *Soc. Neurosci. Abstr.* 19, 106 (1993); V. N. Murthy and E. E. Fetz, *Proc. Natl. Acad. Sci. U.S.A.* 89, 56 (1992); J. N. Sanes and J. P. Donoghue, *ibid.* 9, 4470 (1993).  
 16. For a review of spindling activity, see M. Steriade, G. Jones, R. R. Llinas, *Thalamic Oscillations and Signaling* (Wiley, New York, 1990).  
 17. M. A. L. Nicolelis, R. C. S. Lin, D. Woodward, J. Chapin, *Proc. Natl. Acad. Sci. U.S.A.* 90, 22 (1993); *Nature* 361, 533 (1993).  
 18. R. P. Erickson, *Psychol. Rev.* 75, 447 (1968); P. Churchland and T. J. Sejnowski, *The Computat. Brain* (MIT Press, Cambridge, MA, 1992).  
 19. J. K. Chapin and D. J. Woodward, *Exp. Neurol.* 654 (1982); *ibid.*, p. 870; J. D. Coulter, *J. Neurophysiol.* 37, 831 (1973); R. J. Nelson, *Brain Res.* 31, 143 (1984).  
 20. We thank L. M. O. de Oliveira, L. Andrews, H. W. Gins, G. Hetzel, and A. Kirlov for technical assistance. We thank D. Woodward for comments. This report is dedicated to Cesar Timó-lara. Support by the National Institute of Dental Research (gr DE1121-01), the Whitehall Foundation, and Whitehead Scholar Award to M.A.L.N.; by grants NS-26722 to J.K.C. and NS-29161 R.C.S.L.; and by a doctoral fellowship from the Brazilian government (CAPES 1462-91-2) to L.A.B.

ROUGEUL

EXPLAINS

EXPLAINS MOST OF THE COVARIANCE

and ONR N00014-95-1-

J. K. CHAPIN, EXP. BRAIN RES. 262, 199 (1986)

J. J. BOUYER, M. F. MONTARON, A. ROUGEUL, *IBID* 51, 244 (1981)

PROF. CESAR TIMO-LARA  
PLEASE ADD

31 August 1994; accepted 6 March 1995